Pergamon

Int. J. Heat Mass Transfer. Vol. 40, No. 4, pp. 817–822, 1997

0017-9310/97 $17.00+0.00

PII: S0017-9310(96)00174-3

Control of Rayleigh–Bénard convection in a small aspect ratio container

LAURENS E. HOWLE

Mechanical Engineering and Materials Science Department, Duke University, Durham, NC 27708-0300, U.S.A.

(*Received* 9 *January* 1996 *and in final form* 7 *May* 1996)

Abstract—Active control of Rayleigh–Bénard convection in small aspect ratio horizontal layer, by perturbation of the lower thermal boundary condition, is shown. These experiments use a novel shadowgraphic system to measure the departure of a high Prandtl number fluid from the no-motion state. A proportional control scheme uses the shadowgraphic information as feedback to determine the lower boundary heat flux distribution. An array of individually controlled heaters imposes the heating distribution. Significant suppression of the convection amplitude is possible to at least 10 times the critical Rayleigh number. This convection control method provides an economical alternative to magnetic convection suppression.

INTRODUCTION

A horizontal fluid layer may undergo a bifurcation to Rayleigh–Bénard convection (RBC) when heated from below. The resulting fluid motion greatly enhances heat and mass transfer but may be undesirable or detrimental to some processes such as thermal storage or crystal growth. Methods explored for RBC suppression include; temporal modulation of the thermal gradient [1, 2], superimposed shear flows [3, 4], superimposed horizontal and vertical thermal gradients [5] and micro-gravity [6]. Of these, the terrestrial methods are only marginally successful. Theoretical studies show that a more promising convection control method is active control through perturbation of the thermal or velocity boundary conditions [7–10]. In this paper, I demonstrate that it is possible to suppress RBC in a small aspect ratio container using active feedback control of the lower boundary heat flux. To the best of my knowledge, this is the first time RBC has been actively controlled.

Important parameters for RBC are the reduced Rayleigh number, R, the Prandtl number, Pr and the thermal relaxation time, τ_r. The reduced Rayleigh number is the bifurcation parameter for RBC. Below $R = 1$, the fluid is motionless; under normal circumstances the convection amplitude increases monotonically as R exceeds unity. The ethylene glycol used in this experiment has a Prandtl number of 200. The dimensional vertical thermal diffusion time, $\tau_r = H^2/\alpha = 654$s, where H is the fluid layer height and α is the fluid thermal diffusivity, gives a scale of the time required for the system to respond to a change in the thermal boundary conditions.

EXPERIMENTAL METHOD

The apparatus drawn in Fig. 1 contains the $H = 0.79$ cm high fluid layer. Horizontal aspect ratios of 1×2 are deliberately small to limit the number of possible wave patterns [11] and produce patterns that align preferentially with the short horizontal direction [12]. As a result, the system requires control activation in only one direction in order to suppress longitudinal rolls. The transverse modes, which are not suppressed with this set-up, are not sufficiently excited if R is modest.

The thermal boundary conditions of this system are fixed temperature on the upper boundary and specified flux on the lower boundary. Therefore, the appropriate definition of the Rayleigh number for this experiment is

$$Ra = \frac{g\beta\overline{q''}H^4}{\alpha\nu} \quad (1)$$

where g is the acceleration of gravity, β is the volumetric expansion coefficient of the fluid, α is the thermal diffusivity and ν is the kinematic viscosity. The reduced Raleigh number, R, is found by normalizing Ra with its value at criticality.

To suppress convection, the heaters adjust the spatial distribution of the lower boundary heat flux while keeping the average heat flux, $\overline{q''}$, constant. As a result, the Rayleigh number remains constant. Areas of the lower boundary cooler (warmer) fluid regions receive a greater (lesser) proportion of heating. The heaters are cycled so only one heater is on at any instant. The control cycle, τ_c, is typically two orders of magnitude smaller than τ_r. This control cycle introduces an

NOMENCLATURE

g	acceleration of gravity, gain	β	volumetric expansion coefficient
H	fluid layer height (cm)	ν	kinematic viscosity
I	shadowgraphic intensity	τ	time.
N	number of heaters		
Pr	Prandtl number		
$\overline{q''}$	spatially averaged heat flux	Subscripts	
R	reduced Raleigh number	c	cycle
Ra	Rayleigh number.	i	ith component
Greek symbols		p	proportional
α	thermal diffusivity	r	relaxation time.

unavoidable controller delay. The amount of delay has a direct bearing on the type of control used. For example, increased delay requires the addition of differential control [9].

A shadowgraph measures the average vertical density as a function of the horizontal directions. The shadowgraph's advantage over thermal probes placed in the fluid include making non-invasive measurements and having instantaneous response. A phototransistor array, placed $70H$ from the fluid, measures the shadowgraph intensity at 15 discreet points along the major horizontal direction of the fluid layer. The standard deviation of the shadowgraph intensity gives a measure of the convection amplitude. The Nusselt number is a more common measure of the convection amplitude. However, for this experiment, the measurement bias of the phototransistor data is much smaller than the measurement bias of the thermal transport data which is required to compute the Nusselt number. Eight precision thermistors, four each on the upper and lower boundaries, collect thermal transport data. I conducted several careful experiments with this apparatus to confirm that the present measure of the convection amplitude is proportional to the Nusselt number.

The departure of the local shadowgraphic intensity, I_i, from the mean, $\bar{I}$, and proportional gain, g_p, determine the heating distribution for the next control cycle according to the equation

$$\tau_i = \frac{\tau_c}{N}\left(1 + g_p sgn(I_i - \bar{I})\sqrt{|I_i - \bar{I}|}\right). \tag{2}$$

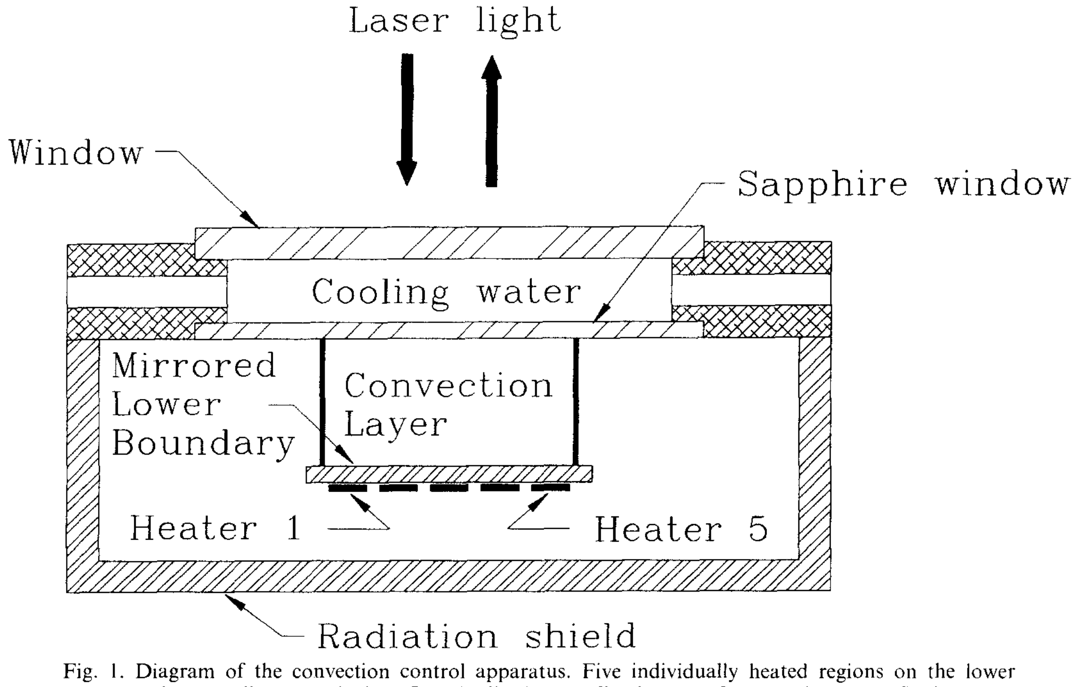

Fig. 1. Diagram of the convection control apparatus. Five individually heated regions on the lower boundary dynamically adjust the heat flux distribution to offset buoyant forces and suppress fluid motion. A shadowgraphic visualization system measures the convection amplitude.

In equation (2), τ_i is the on-time for heater i and N is the number of heaters. Positive gain, g_p, increases the on-time of heaters situated below cooler (than the mean) fluid regions. Conversely, the controller reduces the on-time of heaters below warmer fluid regions.

A 2 mm thick thermally regulated (± 0.005C) sapphire window is the fluid layer upper boundary. The lower boundary is 1 mm thick crown glass, mirrored to provide a reflective surface for the He–Ne laser light used for pattern visualization. Five individual heaters adhere to the underside of the lower boundary and span the short horizontal direction of the enclosure. The segmented lower boundary heating and the lower boundary material are the only components that make this apparatus differ from typical precision convection experiments (see ref. [13], for example).

EXPERIMENTAL RESULTS

Figure 2 (left) shows the uncontrolled ($g_p = 0.0$) convection amplitude vs reduced Rayleigh number, R, near convection onset. The rounding of the bifurcation curve near the critical point is an interesting feature of this plot. In this apparatus, there are slight differences in the lower boundary heating due to non-uniformities in the thermal contact between the heaters and the crown glass lower boundary and other unavoidable experimental imperfections. This can cause heterogeneity in the bifurcation parameter similar to that studied by Zimmermann *et al.* [14] in the one-dimensional Swift–Hohenberg system. Since the Swift–Hohenberg system is a model equation appropriate for convection of high Prandtl number fluids near the onset point, it is a reasonable model for this experiment. Zimmermann *et al.* found localized solutions and rounding in the bifurcation curve similar to the rounding shown in Fig. 2 (left) when they included frozen random fluctuations in the control parameter. This may have a significant impact on convection control in this non-ideal system as I will discuss below.

The first control problem I consider is suppressing convection in the fluid as R increases from subcritical to supercritical values. Figure 2 (right) shows the bifurcation curve R vs amplitude for the case $g_p = 5.0$ and $\tau_c = 10^{-2}\tau_r$ with the uncontrolled case ($g_p = 0.0$) shown as a reference. The figure shows that the convection amplitude is approximately constant at 0.03 in the range $3 < R < 9$. At $R \approx 9$, the fluid motion becomes time-periodic although the average convection amplitude is less than 20% of its uncontrolled value. The convection remains periodic in the range $9 < R < 14$, after which it is no longer suppressed and chaotic convection occurs. Over the range $1 < R < 3$, control is not as successful because the thermal conductivity of the lower boundary smooths out the imposed heat flux profile. Increasing the gain overcomes this problem but at the expense of the high R controllability limit. Ideally, the gain should depend on R and the lower boundary should be thin compared to H.

Theory in the convection control field focuses on the delay of convection onset which is a different problem than convection suppression. For delay of convection onset, one changes the entire bifurcation structure of RBC. Controlled RBC can loose stability through either a supercritical bifurcation to steady convection or a Hopf bifurcation to time-periodic motion,

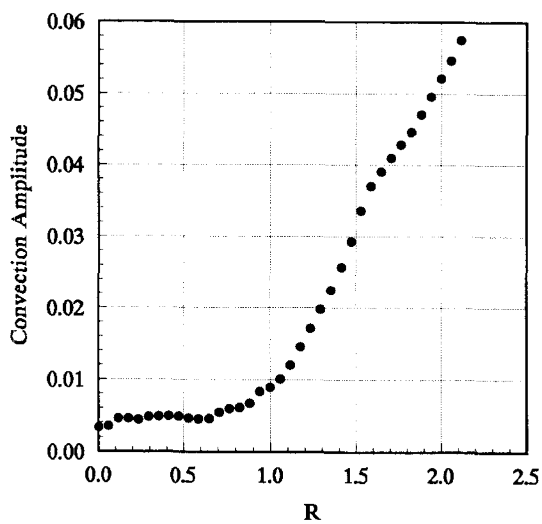

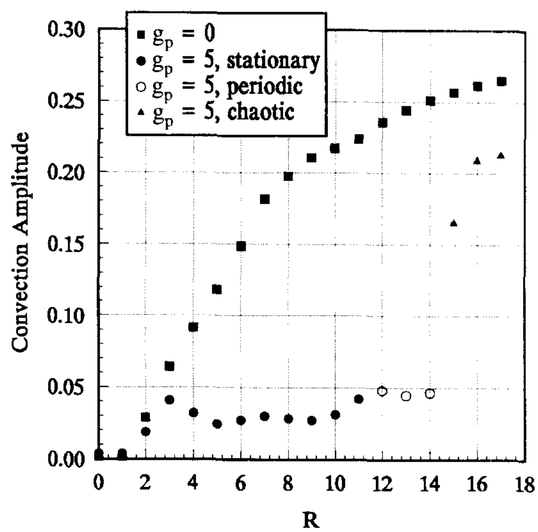

Fig. 2. Uncontrolled bifurcation curve very near the onset of convection (left). The rounding is caused by localized modes in the convection pattern. Convection amplitude for the uncontrolled (squares) and controlled (circles and triangles) cases (right). In this experiment, the reduced Rayleigh number, R, is ramped from 0.0 to 17.0 with and without control. The open circles denote time-periodic convection and the triangles represent chaotic convection. Active control significantly reduces convection over the range $3 < R < 14$. Proportional gain, $g_p = 5.0$, is used for this experiment.

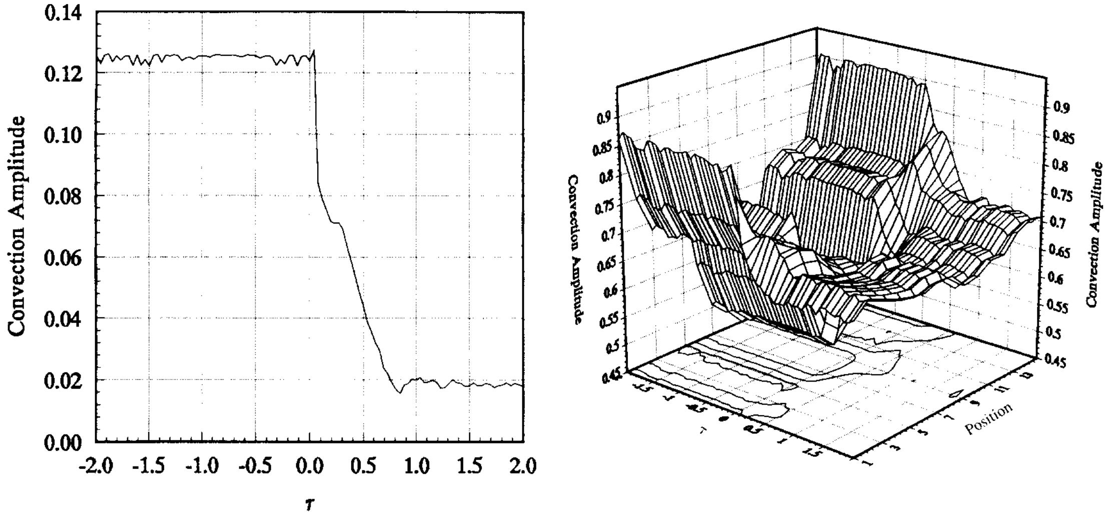

Fig. 3. Convection amplitude (left) and wave pattern (right) as a function of dimensionless time, τ, for $R = 4$. Control with proportional gain $g_p = 12.5$ is switched on at $\tau = 0$. Active control reduces the convection amplitude to 15% of its uncontrolled value.

depending on the Prandtl number and the type and magnitude of control [9]. Figure 2 (right) shows, however, that the convection is not controlled in the context of theory but rather is suppressed. In this system, with its inherent heterogeneity, the idea of convection control by shifting the onset point may be neither possible nor meaningful.

An additional point of interest is the size of the basin of attraction of the controlled problem. Numerical simulations suggest a large basin of attraction [9]. To explore this experimentally, I allow the fluid to relax to a finite amplitude convective state at $R = 4$ with $g_p = 0.0$ (no control) and $\tau_c = 0.04\tau_r$. After transients die out, the computer begins control with $g_p = 12.5$. Figure 3 shows the convection amplitude and wave pattern for $-2\tau_r < \tau < 2\tau_r$. Before $\tau = 0$, the pattern consists of a pair of counter-rotating rolls with warm, up-flowing fluid in the middle of the layer. It takes $0.7\tau_r$ or 18 control cycles to reduce the amplitude to less than 15% of its uncontrolled value. The experiment will require greater heater resolution and control activation in the second horizontal direction to suppress the convection further. A more exhaustive study of the R–g space needs to be completed before the size of the basin is known. This point does show, at least, that the RBC control scheme used here is robust.

As a final experiment, I show that active control is required to suppress the fluid motion to the degree accomplished in these experiments and discuss the controlled heating distribution. This experiment is similar to the previous control experiment except that the controller freezes the spatial flux pattern at the end of the controlled section. Specifically, the controller lets the system relax for $10\tau_r$ with uniform flux then activates and maintains control for $10\tau_r$. Next, the controller freezes the flux at its average spatial distribution. This new flux distribution is used for an additional $10\tau_r$. If the flux distribution rather than active control is responsible for reducing the convection amplitude, then the amplitude will not change after freezing the flux pattern. Conversely, if the active control is responsible for flow suppression, then the convection amplitude will increase. Figure 4 shows the convection amplitude (right) and the heating distribution (left) for this $R = 4$, $g_p = 1.5$, $\tau_c = 10^{-2}\tau_r$ experiment. The amplitude curve, Fig. 4 (left), clearly shows a strong increase in the convection amplitude with the frozen flux pattern, proving that active control is responsible for a major portion of the convection amplitude reduction. The amplitude does not return to the uncontrolled value because the flux pattern (flux concentrated toward both ends of the convection chamber) is not as optimal as the uniform flux pattern. In fact, flux concentrated in the center of the convection layer produces the greatest amplitude. I use this to choose the initial condition and accelerate the thermal relaxation by heating only with the center heater for $\tau_r/5$ before heating the lower boundary uniformly.

In the ideal experiment, the heating should return to a uniform distribution after suppressing the fluid motion [9]. Minor excursions from uniform heating are required thereafter to hold the system on the unstable fixed point. As the right-hand plot in Fig. 4 shows, this is not the case with the present experiment. The difference between these experiments and the ideal case is due to the non-negligible thermal properties of the lower boundary and probably other experimental imperfections such as thermal conduction through the

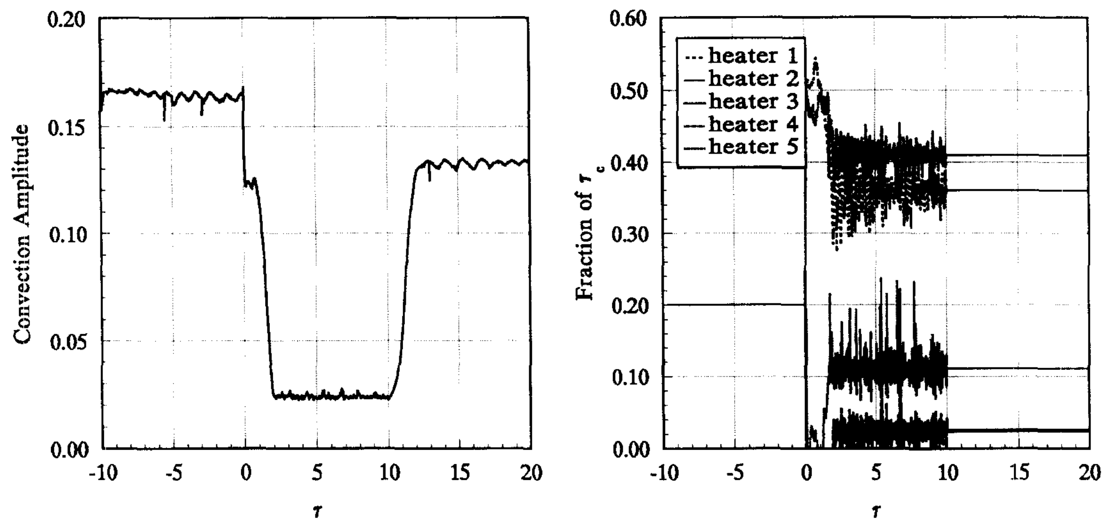

Fig. 4. Convection amplitude (left) and controller actuation (right) at $R = 4$. For this experiment, the system convects with uniform heating for $10\tau_r$; active control with $g_p = 7.5$ is maintained for an additional $10\tau_r$. At the end of the controlled portion of the experiment, the heating distribution is frozen for an additional $10\tau_r$. The increase in the convection amplitude after the heating distribution is frozen proves that active control is needed to hold the convection amplitude to its minimum value.

lateral walls. I also carried out these experiments with a 2 mm thick sapphire lower boundary that has higher thermal conductivity than the crown glass boundaries. Control or suppression of any type is not possible in that system.

CONCLUSION

In this work, I examined active control of convection by perturbation of the flux boundary condition. Since this work included, by necessity, effects such as heterogeneity causing bifurcation rounding, boundary thermal capacitance, a limited number of sensors and actuators, and actuator delay, most of which theoretical studies neglect, it clearly establishes the potential for practical application. Future work should include extending theory to include the effect of the thermal capacity of boundary materials, integration and micro-fabrication of heaters and sensors and nonlinear adaptive control schemes such as neural nets or genetic algorithms. Additionally, recent advances in shadowgraphic visualization make it possible to expand this work to porous media [13] for which some control theory exists [15]. This work also provides an experimental system for control of chaos [16], maintenance of chaos [17], formation of localized solutions in disordered systems [13] and riddled basins of attraction [18].

Acknowledgements—I thank H. H. Bau for several helpful conversations. This work was supported by the Duke University School of Engineering and Mechanical Engineering and Materials Science Department.

REFERENCES

1. Davis, S. H., The stability of time-periodic flows. *Annual Review of Fluid Mechanics*, 1976, **8**, 57–74.
2. Meyer, C. W., Cannell D. S. and Ahlers, G., Hexagonal and roll patterns in temporally modulated Rayleigh–Bénard convection. *Physics Review*, 1992 **45**, 8583–8604.
3. Kelley, R. E., Stabilization of Rayleigh–Bénard convection by means of a slow non-planer oscillatory flow. *Physics and Fluids*, 1992, **4**, 647–648.
4. Kelley, R. E. and Hu, H.-C., The onset of Rayleigh–Bénard convection in non-planar oscillatory flows. *Journal of Fluid Mechanics*, 1993, **249**, 373–390.
5. Ostrach, S. and Raghavan, C., Effect of stabilizing thermal gradients of natural convection in rectangular enclosures. *ASME Journal of Heat Transfer*, 1979, **101**, 238–243.
6. Glicksman, M. E. and Koss, M. B., Dendritic growth velocities in microgravity. *Physics Review Letters*, 1994, **73**, 573–576.
7. Singer, J. and Bau, H. H., Active control of convection. *Physics and Fluids*, 1991, **3**, 2859–2865.
8. Tang, J. and Bau, H. H., Stabilization of the no-motion state in Rayleigh–Bénard convection through the use of active feedback control. *Physics Review Letters*, 1993, **70**, 1795–1798.
9. Tang, J. and Bau, H. H., Stabilization of the no-motion state in the Rayleigh–Bénard problem. *Proceedings of the Royal Society of London, A*, 1994, **447**, 587–607.
10. Tang, J. and Bau, H. H., Stabilization of the no-motion state of a horizontal fluid layer heated from below with Joule heating. *ASME Journal of Heat Transfer*, 1995, **117**, 329–333.
11. Cross, M. C. and Hohenberg, P. C., Pattern formation outside of equilibrium. *Review of Modern Physics*, 1993, **65**, 851–1112.
12. Cross, M. C., Ingredients of a theory of convective textures close to onset. *Physics Review*, 1982, **25**, 1065–1076.
13. Howle, L., Behringer, R. P. and Georgiadis, J., Vis-

ualization of convective fluid flow in a porous medium. *Nature*, 1993, **362,** 230–232.
14. Zimmermann, W., Seesselberg, M. and Petruccione, F., Effects of disorder in pattern formation. *Physics Review*, 1993, **48,** 2699–2703.
15. Tang, J. and Bau, H. H., Feedback control stabilization of the no-motion state of a fluid confined in a horizontal porous layer heated from below. *Journal of Fluid Mechanics*, 1993, **257,** 485–505.
16. Ott, E., Grebogi, C. and Yorke, J. A., Controlling chaos. *Physics Review Letters*, 1990, **64,** 1196–1199.
17. In, V., Mahan, S. E., Ditto, W. L. and Spano, M. L., Experimental maintenance of chaos. *Physics Review Letters*, 1995, **74,** 4420–4423.
18. Ott, E. and Sommerer, J. C., Blowout bifurcations: the occurrence of riddled basins and on-off intermittency. *Physics Review Letters*, 1994, **188,** 39–47.